Gravitational Lensing and the Extragalactic Distance Scale

By ROGER D. BLANDFORD AND TOMISLAV KUNDIĆ

Theoretical Astrophysics, California Institute of Technology, MC 130-33, Pasadena, CA 91125

The potential of gravitational lenses for providing direct, physical measurements of the Hubble constant, free from systematic errors associated with the traditional distance ladder, has long been recognized. However, it is only recently that there has been a convincing measurement of a time delay sufficiently accurate to carry out this program. By itself, an accurate time delay measurement does not produce an equivalently definite Hubble constant and the errors associated with models of the primary lens, propagation through the potential fluctuations produced by the large-scale structure and the global geometry of the universe must also be taken into account. The prospects for measuring several more time delays and the feasibility of making the corresponding estimates of the Hubble constant with total error smaller than ten percent are critically assessed.

1. Introduction

Ever since the prescient work of Refsdal (1964, 1966), extragalactic astronomers have known that a determination of the time delay in the variation of a multiply imaged quasar could produce a measurement of the size and age of the universe. The first definite example of multiple imaging was discovered in the "double quasar" 0957+561A,B (Walsh, Carswell & Weymann 1979), and, as it seemed that this dream might be realized, several groups began monitoring it in the hope of carrying out this program.† It took 17 years for a universally accepted time delay to be measured in this system (Kundić 1996), after a long and controversial series of papers on the subject (for a review, see Haarsma *et al.* 1996). The effort in constraining the models of the lensing mass distribution has paralleled the time delay observations, resulting in a robust model of the system (Grogin & Narayan 1996). Many other promising lenses have been discovered since, and there is now considerable optimism that Refsdal's technique, like many others discussed at this meeting, is ripe for exploitation. In this brief review, we will try to summarize recent developments in the study of gravitational lensing insofar as they are relevant to measurement of the Hubble constant. For more detail on the history and the basic theory, the reader is referred to Blandford & Narayan (1992); Schneider, Ehlers & Falco (1992); and Narayan & Bartelmann (1996). Recent observational and theoretical developments are presented in the 173rd IAU Symposium proceedings (Kochanek & Hewitt 1996).

2. The method

Gravitational lensing relies upon the the propensity of light to follow null geodesics in curved spacetime. This means that if we try to fit the round peg that is the curved space around a mass M into the square hole that is the pre-relativity framework of Euclid, Newton, and Kant, then light rays will appear to be deflected through an angle

$$\hat{\alpha} = \frac{4GM}{bc^2} \tag{2.1}$$

† In fact, they were doing this under false pretenses because the original estimate of the time delay was five times too large, due to an uncharacteristic slip in Young *et al.* (1980).

where b is the impact parameter. Now, an elementary calculation of this deflection angle, analogous to the calculation of the deflection of an ultrarelativistic electron passing by an atomic nucleus, gives precisely half this deflection. When one analyzes the general relativistic calculation, one finds that the other half of the deflection is directly attributable to the space curvature and that this is a peculiar prediction of general relativity. This prediction has been verified with a relative accuracy of ~ 0.001 in a measurement of the solar deflection (Lebach *et al.* 1985) and we can take this part of the theory for granted.

It turns out to be quite useful (and rigorously defensible), to use the Newtonian framework to think in terms of this "deflection" and to treat space as flat but endowed with an artificial refractive index

$$n = 1 - \frac{2\Phi}{c^2}. \tag{2.2}$$

where $\Phi(\vec{r})$ is the conventional Newtonian gravitational potential which $\to 0$ as $r \to \infty$ (Eddington 1919). (As $\Phi < 0$, the refractive index exceeds unity and rays are deflected toward potential wells.) This also implies that when photons travel along a ray, they will appear to travel slower than *in vacuo* and will take an extra time $\Delta t_{\rm grav}$ to pass by a massive object, where

$$\Delta t_{\rm grav} = -\frac{2}{c^3}\int ds\ \Phi \tag{2.3}$$

and where the integral is performed along the ray. (This effect is also known as the "Shapiro delay" and it has been measured with a fractional accuracy ~ 0.002 in the solar system by Reasenberg *et al.* 1979). If the deflector is at a cosmological distance (at a redshift $z_{\rm d}$), the gravitational delay measured by the observer will be $(1 + z_{\rm d})$ times longer, where the expansion factor takes into account the lengthening of time interval proportional to the lengthening of wave periods.

There is a second, geometrical contribution to the total time delay. In order to compute this contribution, it is necessary to take account of the fact that the global geometry of the universe is not necessarily flat. Fortunately, this can be done by defining an *angular diameter distance* (e.g. Weinberg 1972), which is the ratio of the proper size of a small source at the time of emission to the angle that it subtends at a distant observer. (In computing the angular diameter distance, it is necessary to allow for the fact that the universe expands as the light propagates from the source to the observer.) Now define angular diameter distances from the observer to the deflector and the source by $D_{\rm d}$, $D_{\rm s}$ respectively and from the deflector to the source by $D_{\rm ds}$. If we compare the true deflected ray with the unperturbed ray in the absence of the deflector, then elementary geometry tells us that the separation of the two rays at the deflector is given by $\vec{\xi} = D_{\rm d}D_{\rm ds}\vec{\hat{\alpha}}/D_{\rm s}$ (Fig. 1). Now imagine two waves, one emanating from the source at the time of emission, the other emanating from the observer backward in time leaving now and let these two waves meet tangentially at the deflector along the undeflected ray. The extra geometrical path is simply the separation of these wavefronts at the deflector along the deflected ray, a distance $\vec{\xi}$ from the undeflected ray. As the rays are normal to the wavefronts at the deflector, we see that the geometrical path difference at the deflector is just $\vec{\xi}\cdot\vec{\hat{\alpha}}/2$. Again, we must multiply by $(1 + z_{\rm d})$. The net result is an expression for the geometrical time delay

$$\Delta t_{\rm geom} = (1 + z_{\rm d})\frac{D_{\rm d}D_{\rm ds}}{2D_{\rm s}c}\ \hat{\alpha}^2 \quad . \tag{2.4}$$

The total time delay is the sum of the gravitational and the geometrical contributions.

Both the gravitational and the geometrical time delays are of comparable magnitude $\sim \hat{\alpha}^2/H_0$ for cosmologically distant sources. For typical deflections $\sim 1''$, this would

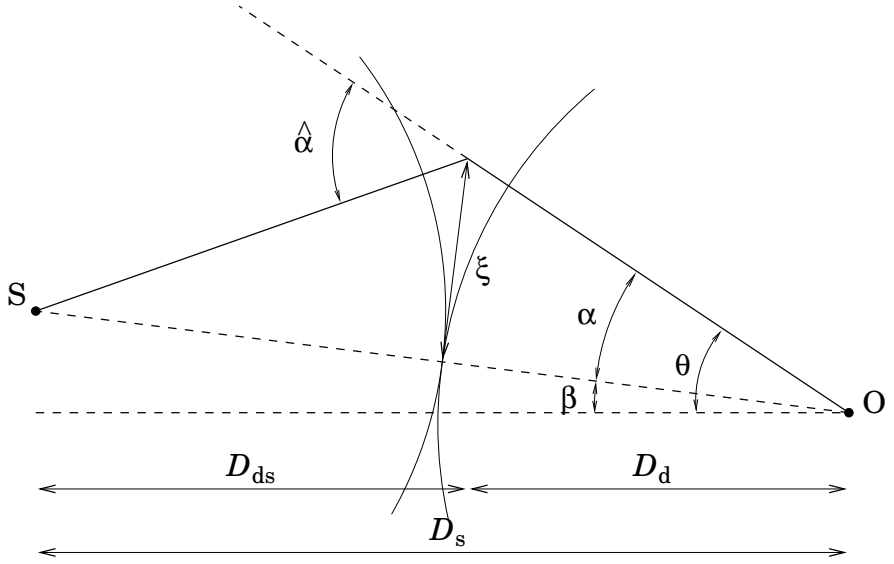

FIGURE 1. Illustration of the geometrical time delay in a simplified lensing geometry. The two wavefronts shown in the figure represent one wave emanating from the source and the other wave emanating from the observer backward in time. They meet tangentially at the deflector along the *undeflected* ray. The separation between these two wavefronts along the *deflected* ray is given by the expression $\vec{\xi}\cdot\vec{\hat{\alpha}}/2$, regardless of the space curvature.

lead to an estimate $\Delta t \sim 1$ yr. Curiously, for many of the sources in which we are most interested, it turns out that the actual delays are much smaller than this estimate (by up to three orders of magnitude). This is because the gravitational and geometrical time delays tend to cancel each other out and because we tend to select observationally highly magnified examples of gravitational lensing in which the image arrangement is quite symmetrical.

In order to evaluate Eqs. 2.3 and 2.4 in a given system, we must construct a model of the deflector. For a general mass distribution, the deflection angle, (which can be regarded as a two dimensional vector as long as it is small), is given by

$$\vec{\hat{\alpha}} = \frac{2}{c^2}\int ds\, \vec{n}\times(\vec{n}\times\boldsymbol{\nabla}\Phi) \tag{2.5}$$

where $\vec{n}$ is a unit vector along the ray. We can now use this deflection to solve for the rays. Let us measure the angular position of the undeflected ray as seen by the observer, relative to an arbitrary origin on the sky, by $\vec{\beta}$ and the position of the deflected ray by $\vec{\theta}$ (Fig. 1). These angles must satisfy the general lens equation

$$\vec{\beta} = \vec{\theta} - \vec{\alpha}(\vec{\theta}) \tag{2.6}$$

where

$$\vec{\alpha} = \frac{D_{\rm ds}}{D_{\rm s}}\,\vec{\hat{\alpha}} \tag{2.7}$$

$\vec{\alpha}$ is the *reduced* deflection angle. When Eq. 2.6 has more than one solution, we have a *strong* gravitational lens producing multiple images. Common strong lenses form two or

four images. We can use use Eq. 2.6 to write the total time delay in the form

$$\Delta t = K\left[\frac{(\vec{\theta}-\vec{\beta})^2}{2} - \Psi(\vec{\theta})\right] \tag{2.8}$$

where

$$K = (1+z_{\rm d})\,\frac{D_{\rm d}D_{\rm s}}{D_{\rm ds}c} \tag{2.9}$$

and

$$\Psi = \frac{2D_{\rm ds}}{D_{\rm d}D_{\rm s}c^2}\int ds\;\Phi \tag{2.10}$$

is the *scaled surface potential* which satisfies the two-dimensional Poisson equation

$$\nabla^2\Psi = \frac{2\Sigma(\vec{\theta})}{\Sigma_c} \quad , \tag{2.11}$$

and where

$$\boldsymbol{\nabla}\Psi = \vec{\alpha} \tag{2.12}$$

is the reduced deflection angle. Σ is the surface density in the lens plane and $\Sigma_c = c^2D_{\rm s}/4\pi GD_{\rm ds}D_{\rm d}$ is the so-called *critical density*. The derivatives are performed with respect to $\vec{\theta}$.

Next, we must calculate the observed magnification. Suppose that we have a small but finite source that is resolved by the observer. In the absence of the deflector, the source will appear at position $\vec{\beta}$ on the sky. After deflection, the β plane will be mapped onto the θ plane. The Hessian tensor

$$H_{ij} = \frac{\partial\beta_i}{\partial\theta_j} = \delta_{ij} - \Phi_{,ij} \tag{2.13}$$

relates the source to the image. (Note that, as the deflection is itself the gradient of a potential, this tensor is symmetric and only has three independent components.) It is usual to relate the image to the source and this requires the *magnification tensor* which is the inverse of Eq. 2.13:

$$\mu_{ij} = \frac{\partial\theta_i}{\partial\beta_j} = H^{-1}_{ij} \quad . \tag{2.14}$$

This magnification tensor can be decomposed into an isotropic *expansion* and a trace-free pure *shear*. As it is symmetric, there is no rotation.

Now the usual scalar magnification, denoted by μ, is the ratio of the flux observed from an unresolved source seen through the deflector to the flux that would have been measured in the absence of the deflector. As the intensity is unchanged by the deflector, this ratio is simply the ratio of the solid angles subtended by the ratio of the flux with and without lensing, given by the Jacobian

$$\mu = \left|\frac{\partial\theta_j}{\partial\beta_i}\right| = |\mu_{ij}| \quad . \tag{2.15}$$

These magnifications are not directly observable. Rather, it is the ratio of the magnifications of separate images of the same source that one measures. (Of course this may have to be done at different times of observation if the source varies so as to make the comparison at the same time of emission.) Similarly, if we are able to resolve angular structure in multiple images of a compact source, for example using VLBI, then we can also measure the relative magnification tensor relating two images, A, B

$$\mu^{AB}_{ij} = \mu^{A}_{ik}(\mu^{B}_{kj})^{-1}. \tag{2.16}$$

This tensor need not be symmetric.

The procedure for estimating the Hubble constant then consists of using the observed positions and magnifications of multiple images of the same source to construct a model of the imaging geometry which allows us to deduce $\vec{\beta}$ for the sources and Ψ for all the images. The total time delay for each image can then be computed in the model up to a multiplicative, redshift-dependent factor K given by Eq. 2.9, which is inversely proportional to H_0. If the time lags between the variation of two (or more) images can be measured, it is then possible to get an estimate of H_0.

3. Measuring time delays

Consider a variable source which produces a variation that can be observed using more than one ray. As the travel time along these rays differs, the corresponding images will vary in brightness at different observing times. If the source is continuously variable, then we should be able to measure the time delay using cross-correlation techniques. The precision with which it can be measured depends on the amplitude and timescale of the source variability, on the frequency of observations and photometric accuracy, and on the value of the time delay itself.

Let us consider optical observations of quasars. Assuming that quasar variability is a stationary process, it can be described in terms of the first-order structure function:

$$V(\tau) = \langle [m(t+\tau) - m(t)]^2 \rangle \quad , \tag{3.17}$$

where $m(t)$, $m(t+\tau)$ are quasar magnitudes recorded at two epochs separated by an interval τ (Simonetti, Cordes & Heeschen 1985). The qualifier "stationary" refers to the assumption that V is not a function of the observation epoch t, but only of the time lag τ between two points on the light curve. In practice, $V(\tau)$ can be well approximated by a power law for time delays between a few days and a few years:

$$[V(\tau)]^{1/2} \sim 0.015 \text{ mag } (\tau/\text{day})^{0.35} \quad , \tag{3.18}$$

where the numerical coefficients were estimated from Press, Rybicki & Hewitt (1992a); Cristiani *et al.* (1996); and from the light curves of several lenses monitored at the Apache Point Observatory. The amplitude of $V(\tau)$ depends on the bandpass and it is larger at bluer wavelengths.

Equation 3.18 illustrates the difficulties associated with measuring short time delays. If the predicted delay is a few days, the expected amplitude of quasar variations is only ~ 0.02 magnitudes, requiring millimagnitude photometry in systems that are often complicated and marginally resolved from the ground (In quadruple lenses, one has to resolve four quasar images in a $\sim 1''$ radius, superimposed on the diffuse light of the lensing galaxy). Even in a resolved system with a much longer time delay, the double quasar 0957+561, there has been much debate about the correct value of the delay, with estimates ranging from ~ 540 days (Lehár *et al.* 1992; Press *et al.* 1992a, 1992b; Beskin & Oknyanskij 1995) to ~ 420 days (Vanderriest *et al.* 1989; Schild & Cholfin 1986; Schild & Thomson 1995; Pelt *et al.* 1994, 1996). Optical data recently acquired at the Apache Point Observatory by Kundić *et al.* (1995, 1996) unambiguously measure a delay of $\Delta t = 417 \pm 3$ days, vindicating the second group. This result required ~ 100 flux measurements in two observing seasons with a median photometric error of $< 1\%$.

A less accurate time delay of 12 ± 3 days has been reported for the radio ring B0218+357 on the basis of radio polarization measurements (Corbett *et al.* 1996). The advantage of the polarization method over direct photometry is that only one parameter (time delay) is needed to align light curves of two images. Alignment of photometric light

curves requires an additional parameter, corresponding to the relative magnification of the two images. More recently, Schechter *et al.* (1996) reported a measurement of two time delays in the quadruple quasar PG1115+080: 23.7 ± 3.4 days between images B and C and 9.4 days between images C and A. Unfortunately, it is not yet possible to model PG1115+080 accurately and so this impressive observation cannot furnish a useful estimate of the Hubble constant at this time. Sources like B1422+231 (Hjorth *et al.* 1996) and PKS1830-211 (van Ommen *et al.* 1995) are also currently being monitored.

4. Modeling strong galaxy lenses

4.1. *The models*

Any estimate of H_0 derived from gravitational lensing will be no better than the lens model that is deduced from observations of the positions and fluxes of the individual images. Lens modeling is, necessarily, a rather subjective business. The procedure that has to be followed depends upon whether or not the images are resolved. In most cases, there are N unresolved point images giving $2(N-1)$ relative coordinates. There are also $(N-1)$ relative fluxes which can be fit to the magnification ratios. Since sources are variable, fluxes must be compared at the same emission time. (A complication that can arise at optical wavelengths is that individual stars in the lensing galaxy can cause additional, variable magnification, called *microlensing*, if the source is sufficiently compact. However, this is unlikely to be a problem at infrared or radio wavelengths.) So, with N point images, there are usually $3(N-1)$ observables which can be used in model fitting. Once the relative time delays in the system are measured, they provide $(N-2)$ additional constraints.

Resolved images contain more information. Firstly, when compact radio sources are resolved using VLBI, the individual images ought to be related by a simple, four parameter, linear transformation (Eq. 2.16). This can be measured and is more useful than the flux ratio alone in constraining the model, and would give an additional $3(N-1)$ observables. Secondly, if the radio structure is large enough, it is possible to expand to one higher order and measure the gradient of μ_{ij}. Thirdly, some sources are so extended that they form ring-like images. This can happen at either radio or optical wavelengths. In this case we have a large number, perhaps thousands of independent pixels to match up. In principle, this can lead to a highly constrained lens (and source) model. The best techniques for tackling this problem at radio wavelengths (Wallington, Kochanek & Narayan 1996) incorporate the model fitting as a stage in the map making procedure and, in some cases this can lead to impressively good models.

In order to model a simple gravitational lens, the scaled potential Ψ of the lensing galaxy, (plus any additional galaxies close enough to contribute to the deflection) is modeled using a simple function that contains adjustable parameters that measure the depth of the potential, its core radius, its ellipticity and its radial variation. A convenient functional form is the *elliptical potential*

$$\Psi_e(\vec{\theta}) = b[s^2 + (1-\gamma_c)x^2 - 2\gamma_s xy + (1+\gamma_c)y^2]^q \tag{4.19}$$

where $\vec{\theta} = (x, y)$ measures distance from the center of the potential which is located at (x_0, y_0). The two parameters γ_c, γ_s combine to describe the ellipticity and the position angle of the major axis. The exponent q measures the radial variation of the density at large radius. A value $q = 0.5$ corresponds to an isothermal sphere and a value $q = 1$ has asymptotically $\Sigma \propto r^{-2}$ as might be appropriate if, for example, mass traces light as in a Hubble profile. The elliptical potential has the advantage that it is quick to compute and good for searches in multi-dimensional parameter space. Its drawback is

that the corresponding surface density is peanut-shaped at large ellipticity. Either two potentials must be superposed to generate realistic surface density distributions or a choice made from a smorgasbord of more complicated potentials (e.g. Schneider *et al.* 1992). In some cases, these potentials can be located and oriented using the observed galaxy image. However, we know that the mass in galaxies does not completely trace the light; in particular it diminishes more slowly with increasing radius. Therefore, we still have some freedom in modeling the mass distribution of lensing galaxies, even if their light profiles are well known. An example of the elliptical potential model is shown in Fig. 2. Motivated by the optical HST images of 1608+656, two elliptical potentials are superimposed to produce the observed quad configuration.

It is also conventional to augment the lensing galaxy potential with a simple quadratic form,

$$\Psi_q(\vec{\theta}) = -\Gamma_c(x^2 - y^2) - 2\Gamma_s xy \quad , \tag{4.20}$$

which is trace-free and corresponds to a pure shear of the images. The external shear has two origins: dark matter lying in the lens plane associated with galaxies outside the strong lensing region and large-scale structure along the line of sight, as we discuss in more detail below.

A common procedure for modeling well observed gravitational lenses is to decide upon a list of independent observables and a smaller number of lens model parameters. These parameters are then varied so as to minimize some measure of the goodness of fit, typically a χ^2 associated with the differences in the observables as predicted by the model from those actually measured. This approach has the merit of rewarding simplicity. However, the fit is usually somewhat imperfect and it is difficult to assign a formal error. A somewhat better approach, that is much harder to implement in practice, is to construct families of more elaborate models that may contain more parameters than observables and which are consequently underdetermined. Using this approach, it ought to be possible to derive many models that exactly recover the observables. We can then assign two types of error to the model time delay. One is associated with the measurement errors in the observables, the other depends upon the freedom in the models and it is here that the outcome depends most subjectively upon what we are prepared to countenance.

4.2. *Modeling "quad" sources*

Let us describe some of the dangers and possibilities involved in model fitting by considering image formation in a simple case, the so-called "quad" sources. These are quadruply imaged point sources formed by a galaxy for which the circular symmetry is broken by an elliptical perturbation. (Depending upon the nature of the potential in the galaxy nucleus, there may also be a fifth, faint, central image which we shall ignore.) For illustration, we use the simplest possible model of a singular isothermal sphere potential perturbed by a quadratic shear, and work to first order in the ellipticity (*cf* Blandford & Kovner 1988).

We write the potential in the form

$$\Psi_s(\vec{\theta}) = \theta_0\theta - \frac{1}{2}\epsilon\theta^2\cos 2\phi \quad , \tag{4.21}$$

where polar coordinates $\vec{\theta} = (\theta, \phi)$ refer to the center of the potential located at the center of the observed lensing galaxy (Fig. 3). The first term $\Psi_s^0 = \theta_0\theta$ describes an isothermal sphere ($\Sigma \propto \theta^{-1}$), and is circularly symmetric. The second term is the non-circular perturbation. We assume that we know its orientation from the shape of the galaxy but treat the ellipticity as unknown. If we set $\epsilon = 0$ and place a source on the axis, then the image will be a circular ring of radius θ_0 known as the *Einstein ring*. We

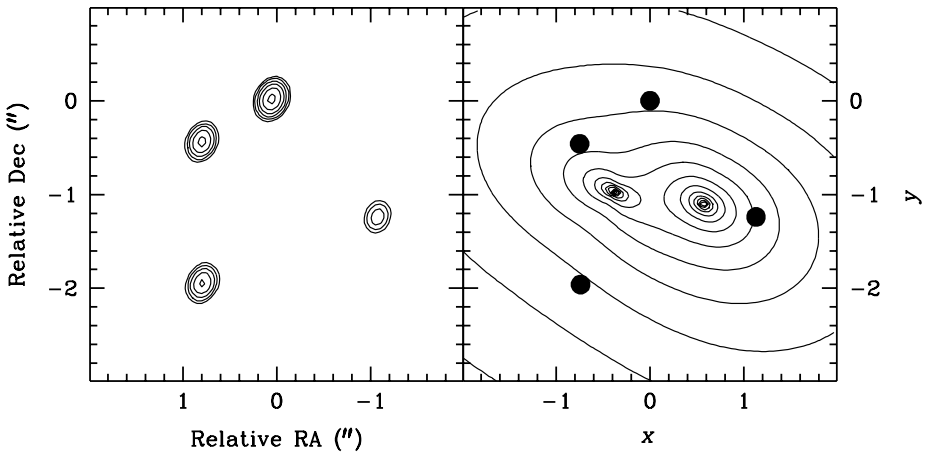

FIGURE 2. **Left:** Radio map of the gravitational lens system 1608+656. The system was observed on 1996 October 10 with the VLA at 8.4 GHz. The map shows four unresolved images of the background source (at $z_s = 1.39$). The brightest image (A) is located at the origin. (Courtesy of Chris Fassnacht.) **Right:** A simple model for 1608+656, consisting of two elliptical potentials. Solid lines represent logarithmically spaced density contours of the lensing mass distribution. The observed image positions (marked with dots) and their relative fluxes are accurately reproduced by this model.

now switch on the perturbation and solve for the source position to linear order assuming that $\epsilon \ll 1$. We find that the source position is

$$\vec{\beta} = [\delta + \epsilon\theta_0 \cos 2\phi]\, \vec{s} - \epsilon\theta_0 \sin 2\phi\, \vec{t} \quad , \tag{4.22}$$

where $\delta = \theta - \theta_0$, and $\vec{s}$, $\vec{t}$ are unit vectors in the radial and tangential directions respectively. We can now evaluate the Hessian and find that its eigenvalues are

$$h_1 = 1 \qquad h_2 = \frac{\delta}{\theta_0} - \epsilon \cos 2\phi \quad , \tag{4.23}$$

and the principal axes are rotated with respect to $\vec{s}$, $\vec{t}$ by an angle

$$\psi = -\epsilon \sin 2\phi \quad . \tag{4.24}$$

These eigenvalues are the reciprocals of the quasi-radial and quasi-tangential magnifications, so that the total magnification is $\mu = (h_1 h_2)^{-1} = (\delta/\theta_0 - \epsilon \cos 2\phi)^{-1}$. The locus of the infinite magnification on the sky, the "critical curve" is then given by $h_2 = 0$ or

$$\delta_c = \epsilon\theta_0 \cos 2\phi \quad . \tag{4.25}$$

The critical curve is the image of the "caustic", the locus in the source plane of points that are infinitely magnified. Its equation is

$$\vec{\beta}_c = [\beta_{cx},\, \beta_{cy}] = 2\epsilon\theta_0[\cos^3\phi,\, -\sin^3\phi] \quad , \tag{4.26}$$

which is the parametric equation of an astroid. If we know the source position, $\vec{\beta}$, and it is located within the astroid then there will be four images located close to the critical curve (Fig. 3). If the source lies outside the astroid, there will be two images.

This model has two free parameters, ϵ and θ_0, and as we may have eleven observables in a four-image lens (three pairs of relative positions + three flux ratios + two time delay ratios), there are many internal consistency checks. For example, the angles of the four

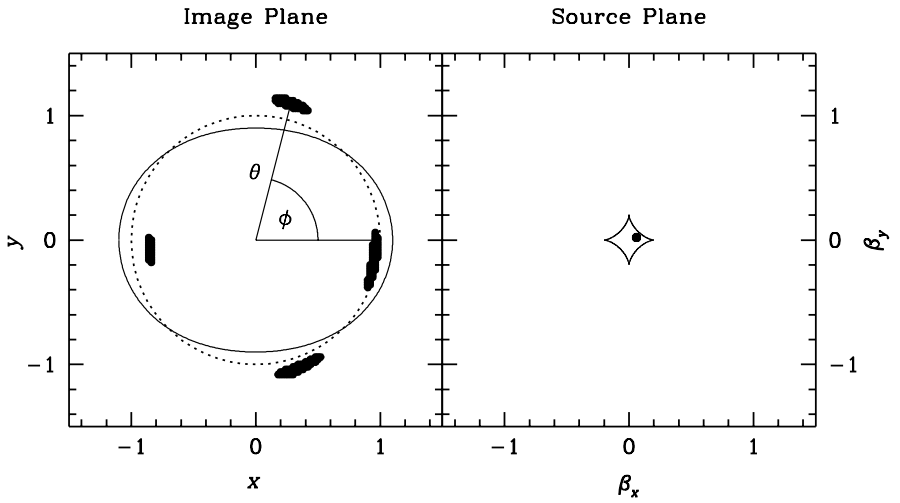

FIGURE 3. Lensing geometry giving rise to a four-image ("quad") configuration. If the source is located within the astroid (diamond) caustic produced by an elliptical potential (right panel), there will be four tangentially elongated images near the critical curve (solid line) in the image plane (left panel). Dotted line in the left panel corresponds to the Einstein ring of the unperturbed, circularly symmetric lens.

images must satisfy

$$\left[\sum_{i=1}^{4}\cos\phi_i\right]^2 = -4\prod_{i=1}^{4}\cos\phi_i \quad . \tag{4.27}$$

Now, in order to trust the model, we contend that it is necessary that every observable be fit within its measurement error, or there should be a good reason why it can be excused. For example, we might have a spectroscopic indication that microlensing is at work in one of the images and then we would discount the measurement of its flux.

Now, it is extremely unlikely that any lens will ever be found that is this simple. So, after we are sure that there is inconsistency, we must introduce additional parameters or change the model. Following the above approach of expanding about the Einstein ring, we can (or may have to) allow the center of the potential to vary, adjust the orientation of the perturbations, allow the ellipticity ϵ to vary with radius θ, introduce higher harmonics (e.g. $\propto \cos 4\phi$ for box-like equipotentials) and so on. Alternatively, we can turn to a density-based model. The nature and quality of the observations will usually dictate this choice.

What we discover when we carry out this procedure is that the allowed range of observables is quite sensitive not just to the parameters, but to the functional form of the model. For example, constraint 4.27 is quite general but can be violated if (not unreasonably) we were to add a $\cos 4\phi$ term. In addition, the shape of the unperturbed, circular potential Ψ_s^0 controls the quasi-radial magnification and changing it changes h_1 to $1 - d^2\Psi_s^0/d\theta^2$. The ratios of time lags are fairly well fixed by the observed image magnifications and location; however, the absolute values (in which we are primarily interested) are extremely sensitive to radial variation of the ellipticity and this can be measured if we have very accurate image positions or an extended source. Finally, we

should probably always include the quadratic form Eq. 4.20 to take account of distant mass.

There are further possible consistency checks. For example, if we can make VLBI observations of the individual image components, as should be possible for 1608+656 (Myers *et al.* 1995, Fassnacht *et al.* 1996; Fig. 2), and resolve structure in the radial direction, we can also check both the radial eigenvalue h_1, and the orientation angle ψ for each of the images. Even better, if we have more than one source, as appears to be the case in 1933+503 (Sykes *et al.* 1996), than we have two independent opportunities to test the model and derive the parameters. (This approach may also be of interest for cluster arcs.)

Let us use the quad H1413+117 for illustration and try to model it using a simple potential (Eq. 4.21). We can guess the lens center pretty accurately, but not the position angle of the major axis of the elliptical perturbation, ϕ_0. Using Eq. 4.27, we find four choices for ϕ_0 and we examine each of these in turn to try to find a consistent solution for the source position $\vec{\beta}$ by varying ϵ, θ_0, and the lens center. We find that none of our choices of ϕ_0 can accomplish this, although one comes close. However, if we now compute the magnification ratios, we find that they are quite inconsistent with the observations. Therefore we can assuredly reject our lens model. It turns out that it is possible to reproduce the positions and fluxes using an elliptical potential with parameters $\{b,\, s,\, q,\, \gamma_c,\, \gamma_s,\, x_c,\, y_c\}$ offset by an external shear with parameters $\Gamma_c,\, \Gamma_s$. Although this seems the most plausible model, it is not unique (Yun *et al.* 1996, preprint) and this would be a concern were this a good choice for monitoring. Unfortunately, it is not as the predicted time delays are almost certainly too small.

4.3. *Uncertainties in the models*

An important question that we must now address is "How do we assign a formal error to the predicted model on the basis of a deflector model?" One procedure is to define a χ^2 using careful values for the measurement errors and then choose parameters p_i that minimize this statistic. We then compute a covariance matrix

$$V_{ij} = \frac{\partial^2 \chi^2}{\partial p_i \partial p_j} \tag{4.28}$$

and invert and diagonalize this quantity so as to form the error ellipsoid. We next compute the maximum fractional change in the time delay within this error ellipsoid and quote this as the fractional error in the derived Hubble constant varying the parameters independently until χ^2/ν increases by unity. The maximum change in the derived value of the delay as we go through this procedure is the required error in the delay.

However, this is still not enough because existence does not imply uniqueness. Suppose that we have a model that truly reproduces all the observables giving an acceptable value for χ^2 and for which the underlying mass distribution is dynamically possible. We should still aggressively explore all other classes of models that can also fit the observations but yet which produce disjoint estimates for the time delay. The true uncertainty in the Hubble constant is given by the union of all of these models. This is a large task. Clearly, we may have to introduce some practical limitations. It is probably quite safe to reject dynamically unreasonable mass distributions, for example positive radial gradients in surface density, but are we allowed to posit isolated concentrations of unseen mass? Of course, only time will tell whether there are genuinely dark galaxies, but until we can demonstrate that all significant perturbers are luminous we must allow for this possibility.

There is already an indication that there may be more unseen mass than we have already included in the discovery that the incidence of quad sources relative to doubles

is much greater than one might have expected if the lenses are about as elliptical as normal galaxies (King & Browne 1996). Three explanations have been advanced for this discrepancy. Firstly, the total mass associated with the observed lensing galaxies may be highly elliptical, or, indeed, quite irregular. (It appears that observed faint galaxies have a median ellipticity of ~ 0.4 as opposed to ~ 0.15 for local galaxies.) Secondly, many of the lenses may actually have unseen companions so that the combined potential will generally be quite elliptical. Thirdly, as we discuss below, propagation effects associated dark matter long the line of sight may actually promote the formation of quads.

4.4. *The double quasar 0957+561*

We now briefly turn from quads to the important case of 0957+561, the only gravitational lens where the time delay has been measured with high accuracy (Kundić *et al.* 1996). Traditionally, 0957+561 was thought to be a difficult system to model because of the small number of constraints in its two-image configuration and because of the complexity of the lensing potential – the primary lensing galaxy G1 is surrounded by a cluster. To a large extent, these problems have been resolved in the extensive theoretical study of Grogin & Narayan (1996). The crucial set of constraints in the GN model was provided by high spatial resolution VLBI mapping of Garrett *et al.* (1994), which resolved inner jets in both images of the source into five centers of emission. Mapping of one jet into the other fixed the relative magnification tensor of images A and B (Eq. 2.16), as well as its gradients along and perpendicular to the jet. This, in turn, provided a tight constraint on the radial mass profile (dM/dr) at the image locations, which, together with the total enclosed mass $M(< r)$, controls the conversion factor between the time delay and the physical distance to the lens. The importance of the dM/dr term was nicely illustrated by Wambsganss & Paczyński (1994).

The remaining model degeneracy in the 0957+561 system between the lensing galaxy G1 and its host cluster cannot be removed by using relative image positions and magnifications (Falco, Gorenstein & Shapiro 1985). It has to be broken by either directly measuring the mass of G1 via its velocity dispersion, or by measuring the surface density in the cluster from its weak shearing effect on the images of background galaxies (e.g. Tyson, Valdes & Wenk 1990, Kaiser & Squires 1993). If both of these parameters are independently determined, they provide an important consistency check on the model.

Falco *et al.* (1996, private communication) recently observed G1 with the LRIS spectrograph at the Keck. Their high signal-to-noise spectrum yields a line-of-sight velocity dispersion roughly in the range $\sigma_{\rm obs} = 275 \pm 30$ km/s (2σ), consistent with the only published measurement by Rhee (1991), $\sigma_{\rm obs} = 303 \pm 50$ km/s. Using a deep CFHT image of the field, Fischer *et al.* (1996) mapped the cluster mass distribution from the distortion of faint background galaxies. Adopting their estimate of the mean background galaxy redshift ($z_{\rm b} = 1.2$) gives the dimensionless cluster surface mass density $\kappa = \Sigma/\Sigma_c = 0.18 \pm 0.11$ (2σ). Using these two results and their measurement of the time delay, Kundić *et al.* (1996) find

$$H_0 = 67^{+10}_{-11} \left(\frac{1-\kappa}{0.82}\right) \ {\rm km\,s^{-1}\,Mpc^{-1}} \tag{4.29}$$

$$= 64^{+13}_{-14} \left(\frac{\sigma_{\rm obs}}{275\,{\rm km\,s^{-1}}}\right)^2 \ {\rm km\,s^{-1}\,Mpc^{-1}} \quad . \tag{4.30}$$

The uncertainty in H_0 is quoted at 2σ and allows for finite aperture effects and anisotropy of stellar orbits in conversion of $\sigma_{\rm obs}$ to G1 mass (GN). While this estimate of H_0 can certainly be improved by future observations, it is already 10% accurate at the 1σ level.

5. Systematic errors

There are a variety of possible systematic errors which afflict gravitational lens determinations of the Hubble constant. The first of these, which we have already mentioned, is the degeneracy between H_0 and a uniform density sheet in the lens plane. For example, suppose that there is a uniform density circular disk of matter covering all the images. This will act like a simple (Gaussian) converging lens and bring the same rays that would have met at the observer to a common focus closer to the lens. In other words, the potential variation is quadratic and so the contribution to the gravitational delay is also quadratic, just like the geometrical delay, from which it is therefore indistinguishable. It has been argued that, as any sheet must have positive mass density, we can only set an upper bound on the Hubble constant (Falco *et al.* 1985).

A second uncertainty is associated with the choice of cosmographic world model. Let us suppose that the universe is of homogeneous Friedmann-Robertson-Walker (FRW) type so that it is parametrized by the current density parameter Ω_0. The angular diameter distances to high redshift sources and lenses depend quite sensitively upon Ω_0. However, the combination $D_{\rm d}D_{\rm s}/D_{\rm ds}$, relevant for the inferred Hubble constant, is relatively insensitive. For example, in the 0957+561 system, $K = 39.9h^{-1}$ days arcsec^{-2} for an Einstein-de Sitter universe with $\Omega_0 = 1$, and $K = 42.9h^{-1}$ days arcsec^{-2} for an open universe with $\Omega_0 = 0.1$. If we take an additional step and introduce a cosmological constant while keeping the universe flat, the change in K is even smaller. For $0 < \Omega_\Lambda < 1$, K attains a maximum of $41.7h^{-1}$ days arcsec^{-2} in the $\Omega_0 = 0.25, \Omega_\Lambda = 0.75$ model. In a lens system with higher redshifts, however, the choice of cosmological model is more important. We can thus use high-redshift lenses to constrain the density parameter Ω_0 once H_0 has been measured. For example, in the $z_s = 3.62$ lensed BAL quasar B1422+231, the difference in K between $\Omega_0 = 1$ and $\Omega_0 = 0.1$ models amounts to 24% (assuming the lens redshift of $z_d = 0.65$, as reported by Hammer *et al.* 1995).

Now let us turn to inhomogeneous cosmological models. If the universe has an overall mean density sufficient to allow it to follow FRW dynamics on the average but with this mass confined to small concentrated lumps, none of which intersect the line of sight, then individual ray congruences will be subject to zero convergence as they cannot pass through any matter. In this case, the angular diameter distance must be changed to the *affine parameter* (Press & Gunn 1973). If, for example, the mass in an Einstein-De Sitter universe were concentrated in large, distant lumps, then K would change by over 10% for B1422+231. However, this assumption is quite unrealistic, because the combined tidal influence of these lumps must, on the average, reproduce the cosmography of a homogeneous universe, and, in fact, it does. In what follows we assume that our line of sight is not special in this sense and that individual dark masses are small enough that we can treat them as smoothly distributed.

The next type of systematic error is starting to be taken more seriously and has broader implications. This is the error introduced in the measurement of H_0 due to large-scale structure distributed along the line of sight from the source to the observer. A simple and standard description of large-scale structure in the universe is to form the power spectrum of relative density fluctuations, $P(k)$, that have supposedly grown from perturbations similar to those that we observe in the microwave background fluctuations. The short wavelength perturbations [$k > k_m \sim (10\ {\rm Mpc})^{-1}$] have grown to non-linear strength; the long wavelength perturbations should still be in the linear regime with $P(k) \propto k$. In the linear regime the potential fluctuations therefore satisfy $\delta\Phi \propto k^{-2}\delta\rho \propto k^{-2}[k^3P(k)]^{1/2} \sim$ constant. In fact, the potential fluctuation is not just constant with linear scale but also

with time and has a value $\delta\Phi \sim 3 \times 10^{-5} c^2$ as normalized to the fluctuations measured by COBE.

The perturbations that are most important for perturbing gravitational lens images are those for which $k^2 P(k)$ is maximized, i.e. with $k \sim k_m \sim (10\ \mathrm{Mpc})^{-1}$. As typical angular diameter distances are $D \sim 1$ Gpc, these subtend angles $\sim 30'$, much larger than the strong lensing regions, and we expect to see $N \sim k_m D \sim 100$ perturbations, of both signs, along the line of sight. If we consider a single ray passing through a roughly spherical perturbation, it will be deflected through an angle $\delta\alpha \sim \delta\Phi/c^2$ and as there are N such deflections adding stochastically, the total deflection will $\delta\theta \sim N^{1/2}\delta\alpha \sim 1'$. (It is amusing that although that there has been so much trouble taken to point HST to a small fraction of a pixel, the universe has a pointing error of about the width of WFPC chip!) In addition, each fluctuation will introduce a propagation time fluctuation $\delta\Phi/k_m c^3 \sim (\delta\Phi/c^2)(D/Nc)$. These fluctuations add stochastically giving a total time difference relative to a homogeneous universe of $\delta t \sim (\delta\Phi/c^2)(D/N^{1/2}c) \sim 10^4$ yr. However, none of this matters because there is no way to detect the deflection or time delay of a single ray.

The situation changes when we consider two rays separated by a small angle θ (Blandford & Jaroszyński 1981). On passing though a single perturbation, the angular separation θ will change by an angle $\sim k_m(D\theta)(\delta\Phi/c^2)$. Again, summing the effects of N such fluctuations stochastically gives an estimate of the total fractional change in θ, a measure of the strength of both the magnification and the shear fluctuations. We obtain

$$\left(\frac{\delta\theta}{\theta}\right) \sim \delta\mu \sim \epsilon \sim \frac{\delta\Phi}{c^2} N^{3/2} \sim 0.03 \quad . \tag{5.31}$$

These fluctuations should be coherent over angles $\sim (1/k_m D) \sim 30'$ on the sky. There have been attempts to measure this signal using the images of faint galaxies (e.g. Mould *et al.* 1994).

There is a subtlety when we consider the observable time fluctuations. If the separation of a pair of rays θ is much less than the angular scale of the fluctuation, we can Taylor expand the potential. We have already dismissed the constant term and might expect the linear term to be observable. However, this is not the case as can be seen by noting that its effect simply deflects both rays through the same angle, just like a prism, and does not increase the optical path at all. We have to expand Φ to quadratic order across the rays to obtain a total time difference due to the fluctuations of $\delta t \sim (\delta\Phi/c^2)(D/N^{1/2}c)(k_m\theta D)^2 \sim (\delta\Phi/c^2)N^{3/2}(D\theta^2/c)$. Now suppose that these two rays are associated with a common source and observer in a gravitational lens. The time delay in an otherwise homogeneous universe would be $t \sim D\theta^2/c$ and so the relative change in the arrival time will satisfy

$$\left(\frac{\delta t}{t}\right) \sim \frac{\delta\Phi}{c^2} N^{3/2} \sim 0.03 \quad , \tag{5.32}$$

as above. Therefore to order of magnitude, we find that a few percent error in the derived value of the Hubble constant will be introduced by the effects of large-scale structure and the effect deserves computing seriously.

This problem has been addressed by Seljak (1994) and Bar-Kana (1996), following earlier papers by Kovner (1987) and Narayan (1991). They find three distinct effects:

(*a*) The images of the source, their positions and their shapes, are subject to a global shear transformation. This effect will generally be absorbed in the quadratic contribution to shear from the large-scale distribution of mass in the deflector plane.

(*b*) The images of the deflecting galaxies, their positions relative to the images of the

source and their shapes will be subject to an additional shear. Naturally this shear is only caused by fluctuations between us and the deflector. This effect means that there is a cosmic uncertainty in the image positions which must be taken into account when we make the models.

(c) There will be quadratic potential fluctuations acting on the unperturbed rays that cause stochastic gravitational delays that create additional direct changes in the measured lags. These will translate directly into errors in H_0. There is an interesting observational possibility here. We can contemplate performing deep redshift surveys in the vicinity of the most promising lenses and rather than treat these effects as random errors, try to remove them directly.

6. Is a ten percent measurement of H_0 attainable?

In order for a gravitational lens measurement of H_0 to be of primary importance, it is probably going to be necessary for it to have an accuracy ~ 10 percent. Is this realistically attainable? Firstly, we can say that it is possible to measure the time delay to better than seven percent accuracy as demonstrated by the optical observations of 0957+561. This should be repeatable in other selected sources. However, accuracies this good have yet to be demonstrated at radio wavelengths, partly because variations over the expected time delays have smaller amplitude. It is prudent to take into account such factors as the expected delay (neither too short nor too long), the signal-to-noise ratio in individual flux measurements, and a measured structure function before deciding which few sources to monitor regularly. Simulations should be used for deciding how frequently to measure the flux.

Secondly, we need to be able to model the lenses with a total fractional uncertainty in the predicted time delay also below ~ 7 percent. Here, there are two challenges. As we have discussed, the model itself must be constrained so well that we are confident that there are no other models of the deflector that recover all the observables to within the measurement errors and yet predict seriously different delays. In addition, we must convince ourselves that the perturbative effects of the large-scale structure along the line of sight do not influence our result at this level.

There is a plethora of alternative schemes to measure H_0, and each one of them has enthusiastic advocates. In this competitive environment, all methods carry a burden of proof and must demonstrate a reliability and reproducibility if they are to become widely accepted. In the particular case of gravitational lenses, this means that we must derive consistent values of the Hubble constant in several, probably at least four, cases. It is also probably necessary for the models to be specified and analyzed prior to measuring the time delay. The considerations outlined above suggest that this goal is attainable and, as the gravitational lens method is directly physical and free from the calibration uncertainties that bedevil most other methods it is well worth the observational effort to carry out this program.

We acknowledge support under NSF grants AST 92-23370 and AST 95-29170. Support for this work was also provided by NASA through grant number AR-06337.15-94A from the Space Telescope Science Institute, which is operated by the Association of Universities for Research in Astronomy, Inc., under NASA contract NAS5-26555. We thank Ed Turner, David Hogg and the whole CLASS collaboration, especially Ian Browne, Chris Fassnacht, Sunita Nair and Tony Readhead, for discussions.

REFERENCES

Bar-Kana, R. 1996, *ApJ*, **468**, 17.

Beskin, G. M., & Oknyanskij, V. L. 1995, *A&A*, **304**, 341.

Blandford, R. D., & Jaroszyński, M. 1981, *ApJ*, **246**, 1.

Blandford, R. D., & Kovner, I. 1988, *Phys. Rev. A*, **38**, 4028.

Blandford, R. D., & Narayan, R. 1992, *ARA&A*, **30**, 311.

Corbett, E. A., Browne, I. W. A., Wilkinson, P. N., & Patnaik, A. R. 1996, in *Astrophysical Applications of Gravitational Lensing* (eds. C. S. Kochanek & J. N. Hewitt) Dodrecht: Kluwer, 37.

Cristiani, S., Trentini, S., La Franca, F., Aretxaga, I., Andreani, P., Vio, R., & Gemmo, A. 1996, *A&A*, **306**, 395.

Eddington, A. S. 1919, *The Observatory*, **42**, 119.

Falco, E. E., Gorenstein, M. V., & Shapiro, I. I. 1985, *ApJ*, **289**, L1.

Fassnacht, C. D., Womble, D. S., Neugebauer, G., Browne, I. W. A., Readhead, A. C. S., Matthews, K., & Pearson, T. J. 1996, *ApJ*, **460**, L103.

Fischer, P., Bernstein, G., Rhee, G., & Tyson, J. A. 1996, *AJ*, in press (preprint astro-ph/9608117).

Garrett, M. A., Calder, R. J., Porcas, R. W., King, L. J., Walsh, D., & Wilkinson, P. N. 1994, *MNRAS*, **270**, 457.

Grogin, N. A., & Narayan, R. 1996, *ApJ*, **464**, 92 (GN).

Haarsma, D., Hewitt, J. N., Lehár, J., & Burke, B. F. 1996, *ApJ*, submitted (preprint astro-ph/9607080).

Hammer, F., Rigaut, F., Angonin-Willaime, M.-C., & Vanderriest, C. 1995, *A&A*, **298**, 737.

Hjorth, J., Jaunsen, A. O., Patnaik, A. R., & Kneib, J.-P. 1996, in *Astrophysical Applications of Gravitational Lensing* (eds. C. S. Kochanek & J. N. Hewitt) Dodrecht: Kluwer, 343.

Kaiser, N., & Squires, G. 1993, *ApJ*, **404**, 441.

King, L. J., & Browne, I. W. A. 1996, *MNRAS*, **282**, 67.

Kochanek, C. S., & Hewitt, J. N. 1996, *Astrophysical Applications of Gravitational Lensing*, Dodrecht: Kluwer.

Kovner, I. 1987, *ApJ*, **316**, 52.

Kundić, T., Colley, W. N., Gott, J. R. III, Malhotra, S., Pen, U., Rhoads, J. E., Stanek, K. Z., & Turner, E. L. 1995, *ApJ*, **455**, L5

Kundić, T., *et al.* 1996, *ApJ*, submitted (preprint astro-ph/9610162).

Lebach, D. E., Corey, B. E., Shapiro, I. I., Ratner, M. I., Webber, J. C., Rogers, A. E. E., Davis, J. L., & Herring, T. A. 1995, *Phys. Rev. Lett.*, **75**, 1439.

Lehár, J., Hewitt, J. N., Roberts, D. H., & Burke, B. F. 1992, *ApJ*, **384**, 453.

Mould, J., Blandford, R., Villumsen, J., Brainerd, T., Smail, I., Small, T., & Kells, W. 1994, *MNRAS*, **271**, 31.

Myers, S. T., *et al.* 1995, *ApJ*, **447**, L5.

Narayan, R. 1991, *ApJ*, **378**, L5.

Narayan, R., & Bartelmann, M. 1996, in *Formation of Structure in the Universe* (eds. A. Dekel & J. P. Ostriker) Cambridge: Cambridge University Press (preprint astro-ph/9606001).

Pelt, J., Hoff, W., Kayser, R., Refsdal, S., & Schramm, T. 1994 *A&A*, **286**, 775.

Pelt, J., Kayser, R., Refsdal, S., & Schramm, T. 1996, *A&A*, **305**, 97.

Press, W. H., & Gunn, J. E. 1973, *ApJ*, **185**, 397.

Press, W. H., Rybicki, G. B., & Hewitt, J. N. 1992a, *ApJ*, **385**, 404.

Press, W. H., Rybicki, G. B., & Hewitt, J. N. 1992b, *ApJ*, **385**, 416.

Reasenberg, R. D., *et al.* 1979, *ApJ*, **234**, L219.

Refsdal, S. 1964, *MNRAS*, **128**, 295.

Refsdal, S. 1966, *MNRAS*, **132**, 101.

Rhee, G. 1991, *Nature*, **350**, 211.

Schechter, P. L., *et al.* 1996, `http://arcturus.mit.edu/~schech/pg1115.html`.

Schild, R. E., & Cholfin, B. 1986, *ApJ*, **300**, 209.

Schild, R. E., & Thomson, D. J. 1995, *AJ*, **100**, 1771.

Schneider, P., Ehlers, J. & Falco, E. E. 1992, *Gravitational Lenses*, Heidelberg: Springer.

Seljak, U. 1994, *ApJ*, **436**, 509.

Simonetti, J. H., Cordes, J. M., & Heeschen, D. S. 1985, *ApJ*, **296**, 46.

Sykes, C. M., *et al.* 1996, *MNRAS*, submitted.

Tyson, J. A., Valdes, F., & Wenk, R. A. 1990, *ApJ*, **349**, L1.

van Ommen, T., Jones, D., Preston, R., & Jauncey, D. 1995, *ApJ*, **444**, 561.

Vanderriest, C., Schneider, J., Herpe, G., Chevreton, M., Moles, M., & Wlérick, G. 1989, *A&A* **215**, 1.

Walsh, D., Carswell, R. F., & Weymann, R. J. 1979, *Nature*, **279**, 381.

Weinberg, S. 1972, *Gravitation and Cosmology*, New York: Wiley.

Wallington, S., Kochanek, C. S., & Narayan, R. 1996, *ApJ*, **465**, 64.

Wambsganss, J., & Paczyński, B. 1994, *AJ*, **108**, 1156.

Young, P., Gunn, J. E., Kristian, J., Oke, J. B., & Westphal, J. A. 1980, *ApJ*, **244**, 736.